FUDMA Journal of Sciences (FJS)
ISSN online: 2616-1370
ISSN print: 2645 - 2944
Vol. 8 No. 2, April, 2024, pp 204 - 211
DOI: https://doi.org/10.33003/fjs-2024-0802-2347

PREPARATION AND CHARACTERIZATION OF BENTONITE CLAY CATALYSTS FOR TRANSESTERIFICATION OF WASTE COOKING OIL INTO BIODIESEL

***Faruk Usman and Muhammed Alkali**

Department of Pure and Industrial Chemistry, Faculty of Science, Federal University Birnin Kebbi, P.M.B. 1157, Nigeria

*Corresponding authors' email: faruk.usman@fubk.edu.ng

ABSTRACT

The development of low-cost green catalytic materials is crucial for the conversion of non-edible vegetable oils or waste materials into biodiesel. The research focuses on the preparation and characterization of aluminium pillared clay and NaOH-doped bentonite clay catalysts for biodiesel production from waste cooking oil using XRF, XRD, FTIR and N_2 adsorption-desorption techniques. The molecular profile and functional group assessment of the biodiesel were done using GC-MS and FTIR respectively. XRF analysis revealed the presence of oxides in all samples. The amount of SiO_2 in all samples was within the range of 35.303–39.199 wt%. Al_2O_3 increased from 15.560 to 19.11 wt%, while the interlayer cations decreased after pillaring. FTIR revealed the appearance of peaks which are characteristic of bentonite. The pillaring and impregnation of NaOH with bentonite led to a distortion of certain peaks' intensity, as evidenced by FTIR results. The pillaring caused an increase in BET surface area and pore volume compared to bentonite from 302.1 to 366.4 m2/g, and 0.186 to 0.189 cc/g respectively, while a decrease in surface area and pore volume was observed in NaOH/bentonite due to impregnation. The XRD data have shown the increase of basal d-spacing of pillared clay from 12.65 to 16.49 Å relative to bentonite with a decrease to 12.45 in the case of NaOH/bentonite. The catalysts prepared outperformed neat bentonite with NaOH/bentonite, resulting in the highest yield of (83 ± 1.80). GC-MS, FTIR, and physicochemical analyses confirmed the production of fatty acid methyl esters.

Keywords: Bentonite, Pillared clay, Biodiesel, Waste cooking oil, NaOH/Bentonite

INTRODUCTION

The depletion of petroleum reserves and the rise in oil prices are problems that have always been associated with fossil energy. To meet the tasks of energy availability, it is required to utilize the enormous potential of renewable energy sources (Rahadianti *et al*., 2018). Biodiesel is another source of energy that can be harnessed in Nigeria. This biofuel has become a global issue due to its merits over conventional diesel, such as a noteworthy decrease in emission of greenhouse gases, cetane number, flash point and lubricity characteristics, biodegradability, and renewability, with no significant difference in the heat of combustion of these fuels (Banerjee *et al*., 2014). Furthermore, biodiesel returns approximately 90% more energy than the energy used to produce it (Farooq *et al*., 2015). Because of these advantages, biodiesel is now used worldwide (Abdul Raqeeb and Bhargavi, 2015) because it can run any existing conventional compression ignition engine if mixed in different proportions. The large-scale production and utilization of biodiesel is hindered by the exorbitant cost of production. In comparison with petroleum diesel, the cost of feedstock oils, and limited edible and non-edible oils are also contributing factors because 70-95% of the whole cost of production is related to raw materials (Saini, 2017). An alarm has been raised over fear that food supply may compete with edible vegetable oils and fats used for biodiesel production (Saini, 2017). Feedstock such as waste cooking oil can help in overcoming the issues raised and even reduce the costs by 60-70 percent (Zhang *et al*., 2012). Waste cooking oil (WCO) originates from a variety of sources, including domestic, commercial, and industrial sources. (Farouq *et al*., 2015). Acid-catalyzed transesterification is required when inedible oils and waste materials are used for the production due to high free fatty acids (Hamzah *et al*., 2021). Supported catalysts have always been introduced because they have high catalytic element thermostability and intercropping distribution (active surface volume) (Liu and Corma, 2018). Abundance, non-hazardous, enhancement of faster rate at lower temperatures during reactions, ease of separation and recovery are among the main reasons clays are referred to as green catalytic materials. Montmorillonite which is the main constituent of bentonites and belongs to the smectite group of clays is now attractive to researchers. (Kurian and Kavitha, 2016). Pillaring is a process that increases the catalytic activity of bentonites. During this process, strong oxide particles are formed between the clays.

Recently, it was reported that neat bentonites can be used as catalysts or supports for transesterification reactions. Nevertheless, there is little evidence available on its comparison with NaOH-impregnated bentonite and superior pillared bentonite as a support or catalyst for producing biodiesel. As a result, the focus of this work is to use waste cooking oil as feedstock for the production of biodiesel using raw bentonite, NaOH-impregnated bentonite, and pillared bentonite as catalysts. Because of the abundance and low cost of bentonite and waste cooking oil, this study provides a more environmentally friendly and cost-effective method for producing biodiesel.

MATERIALS AND METHODS

Chemicals Used

The solvent and chemicals utilized include methanol (95.5 % Sigma), sodium hydroxide (95%, Sigma), aluminium chloride (95 % BDH), silver nitrate (BDH), bentonite (Sigma), potassium hydroxide (99 % BDH), hydrochloric acid (36 % BDH), and sodium thiosulphate (Qualikems). All chemicals were obtained without further purification.

Sample Collection and Preparation

The waste cooking oil used in this study was obtained from major restaurants in Birnin Kebbi, Kebbi State, Nigeria. To remove moisture, the samples were heated in a beaker at 110 ˚C for 30 minutes. Room temperature was used to cool the WCO sample and then all food residues and suspended solids

were removed by filtration. The filtered WCO samples were kept in a sealed container (Tadesse *et al*., 2019).

Methods

Preparation of the catalysts

Preparation of pillared clay

$AlCl_3$ (100 cm^3 of 0.25 M) solution was placed in a beaker followed by the slow addition of 1 M NaOH until OH/metal = 2 (50 cm^3 of the NaOH). The solution was mixed at room temperature and allowed to age overnight at 60 °C. The pillaring solution was mixed with a suspension of clay (5%) to achieve 20 meq of Al^{3+}/g of clay. The mixture was positioned in an ultrasonic bath (50 kHz) at ambient temperature (300 K) for 20 min. The product was centrifuged (4500 rpm, 5 min) and washed with water (20 cm^3/g x5) or use $AgNO_3$ test to confirm the removal of chloride ions. The material was dried at 60 °C for 4 h and then ground to >40 mesh. The intercalated materials were calcined (500 °C for 6 h) in a programmable furnace (10ºC/min) (Suhas *et al*., 1999; Trombetta *et al*., 2000). The resultant material was labelled Al-PILC.

Preparation of NaOH/bentonite

The bentonite was modified through the impregnation method. Sodium hydroxide (1.0 M) and bentonite at a 1:20 ratio were transferred into a round-bottom flask with three necks which was equipped with a thermometer, stirrer and condenser. The mixture was stirred and heated for 24 hr at 60 °C. The material obtained was oven-dried for 24 hr at 70 °C. A Muffle furnace at 400°C for 3 hr was used to calcine the final material (Hamzah *et al*., 2021). The resulting material was labelled NaOH/bentonite.

Characterization of the Catalysts

Surface Area and Pore Volume Analysis

The pore volume and surface area analysis of the neat bentonite and NaOH/bentonite were examined by N_2 adsorption isotherms at 77.35 K using the Quantachrome machine (Version 11.03). The samples were vacuum-degassed for three hours at 250 °C. Multipoint Brunauer-Emmett-Teller (BET) was used to compute the surface area while Barrett-Joyner-Halenda (BJH) method was used to compute the pore volume and size (Collin *et al*. 2015).

FTIR Analysis

FT-IR analysis was performed at Usmanu Danfodiyo University's Central Advance Science Laboratory Complex (CASLAC) in Sokoto using an FT-IR spectrometer (Agilent Cary 630) equipped with a high infrared radiation emission base system. 5-bounce diamond ATR sampling accessories in combination with the base system were used. transmittance mode, with the signal collected between 4000-650 cm^{-1} wavenumbers was utilized for the examination. The samples scan and background scan were both 32 at a resolution of 4. The sample spectra were generated using the Microlab software.

XRD and XRF Analyses

Rigaku MiniFlex 6G with Rigaku SmartLab software was used to perform the Powder X-ray Diffraction (PXRD) analysis at Usmanu Danfodiyo University's Central Advance Science Laboratory Complex (CASLAC) in Sokoto. The measurements were performed with Cu-Kα radiation (40 kV, 15mA) using an Sc-70S detector and recorded over a 3-90° 2 range at a speed of 10.00º/min. XRF analysis was performed using an EDXRF analyzer at the Advanced Science Central Laboratory, Umaru Musa Yar'adua University, Katsina.

Transesterification of Waste Cooking Oil

A three-neck round-bottom flask was used for the reaction. WCO (50 g) sample was placed in the flask along with 0.5 wt% bentonite catalysts dissolved in a 9:1 methanol to oil molar ratio. Previous research demonstrated that using only catalyst at 0.5wt% and a methanol to oil molar ratio of 9:1 were sufficient. The mixture in the flask was heated for 1 hr at 55 °C in a controlled water bath. The catalyst was separated from the mixture using a centrifuge and the remaining mixture was allowed to settle for 12 hr. The bottom layer which is the glycerol (bottom layer) was removed while the biodiesel (upper layer) was further purified. Purification was performed with hot water (above 70°C) to a pH of 7. 1.1 ratio was used as the ratio of the hot water and biodiesel. A hot plate was used to heat (110°C) the biodiesel for 10 mins to remove the remaining moisture (Hamzah *et al*., 2021).

Biodiesel Assay

Determination of Molecular Profile and Functional Group Assessment of Biodiesel

The biodiesel samples were characterized by gas chromatography mass spectrometry. A heating rate (10 ˚C/min) and a split ratio of 1:0 was operated (1 min at 80 °C) until 200 ˚C was obtained and held for 4 min. It was then heated (10 °C/min) to reach 280 °C and held for 5 min. A mass spectrophotometer (quadrupole) was used for the detection which was equipped with a 70eV electron impact ion generator operating in the range of 40-450 m/z. A signal/noise ratio of 5 was used in the total ion chromatography. The percentage peak areas were used to compute the different compositions present. The National Institute of Standards and Testing (NIST) Library was used to identify the fraction peaks obtained from the mass spectra. The biodiesel yield was determined by comparing the peak areas (%) of the obtained spectra Agilent Cary 630 FT-IR spectrometer was used to perform the FT-IR analysis. It operated in the range of 4000-650 cm^{-1} with a resolution of 4 cm^{-1}. This investigation helped to recognize the functional groups present in the biodiesel produced.

Determination of Physicochemical Properties of Biodiesel

Acid, saponification, and iodine values were determined using equations 1-3 (AOCS, 2016). The viscosity was analyzed using ASTM D 445. The estimation of Cetane number (CN) was done using equation 4 (Gopinath *et al*., 2015; Galadima *et al*., 2022) while the estimation of high heating value (HHV) was done using equation 5 (Muhammad *et al*., 2016).

$$Acid\ value = \frac{V \times M \times 56.1}{W} \ldots \quad (1)$$

V= Volume of standard KOH solution in cm^3

M=Molarity of standard KOH solution.

W=Weight of oil sample in grams

$$Saponification\ value = \frac{(B-T) \times M \times 56.1}{W} \ldots\ldots \quad (2)$$

B= cm^3 of HCl required by blank

T= cm^3 of HCl required by oil sample

M= Molarity of HCl

W=Weight of oil in g

$$Iodine\ value = \frac{(B-A) \times M \times 12.7}{W} \ldots \quad (3)$$

B = cm^3 of 0.1 M $Na_2S_2O_3$ required by blank

A = cm^3 of 0.1 M $Na_2S_2O_3$ required by oil sample

M = Molarity of $Na_2S_2O_3$

W = Weight of oil in g

$$CN = 46.3 + \frac{5458}{SV} - 0.225IV \ldots\ldots \quad (4)$$

$$HHV = 49.43 - (0.041\ SV + 0.015\ IV) \ldots \quad (5)$$

RESULTS AND DISCUSSION

Table 1: Result of elemental composition of bentonite, Al-PILC and NaOH/Bentonite

Oxides	Bentonite	Al-PILC	NaOH/Bentonite
Al_2O_3	15.560	19.911	14.764
SiO_2	39.199	35.303	38.275
Fe_2O	8.192	7.747	7.082
MgO	3.210	3.790	3.330
K_2O	1.197	0.791	1.077
CaO	0.482	0.048	0.406
NaO	0.000	0.000	5.230
TiO_2	2.050	1.543	1.980
MnO	0.173	0.190	0.171

The oxides present in bentonite, AL-PILC, and NaOH/bentonite are presented in Table 1. SiO_2 had the highest content in all the samples analyzed as clearly shown in the table and is consistent with the result reported by Daroughegi *et al*. (2018), Elfady *et al*. (2017), and Moma *et al*. (2018) reported higher contents of SiO_2 and Al_2O_3 in their works. Al_2O_3 and SiO_2 are major constituents of bentonite and kaolinite. A high content of montmorillonite is expected due to the appearance of Al_2O_3 in a high amount. cristobalite mineral impurities are linked to Silica (SiO_2). (Daroughegi *et al*., 2018). Both SiO_2 and Al_2O_3 are important clay components. The bentonite has a CaO content of 0.48 (wt%) but Na_2O was not detected; therefore, the bentonite herein is classified as Ca-montmorillonite. In addition to Ca^{2+}, bentonite contains K^+ and Mg^{+2} as cations existing between the layers and can be substituted by Al^{3+} from the pillaring solution. The amount of these interlayer cations was significantly reduced after pillaring, indicating their replacement with Al^{3+}. The Al_2O_3 content of 15.56 (wt %) was increased to 19.911 (wt%) after pillaring, as indicated in the Al-PILC results. After the impregnation of the bentonite with NaOH, Na_2O (5.230 wt%) was observed in the NaOH/Bentonite sample indicating successful doping of Na_2O

Table 2: Result of FTIR Analysis of the samples

Samples	Stretching of Al-OH	Deformation of Al-OH	Stretching of OH of water	Deformation of OH of water	Stretching of Si-O	Deformation of Al-Mg-OH
Bentonite	3623	915	3408	1638	984	793
Al-PILC	3623	907	3405	1627	997	800
NaOH/Bentonite	3617	907	3400	1627	984	793

Figures 1-3 show the spectra of all samples studied. Table 2 contains the assignments and wavenumbers of the major bands, which are in agreement with previous reports (Daroughegi *et al*., 2018; Elfady *et al*., 2017; Moma *et al*., 2018). The bands around 3400, 1620, 3630, 920, 1000 and 800 cm^{-1} correspond to the stretching of OH of water, deformation of OH of water, Stretching of Al-OH, deformation of Al-OH, stretching of Si-O, and deformation of Al-Mg-OH, respectively (Zhao *et al*., 2010). These assignments identify the samples as bentonite clay (Ofoegbu-Chibuzo *et al*., 2022). The interlayer cations were substituted by the metal pillars and that act caused the reduction of water present in the interlayer water. This in turn causes the increase in the width of the peak around 3400 cm^{-1} in Al-PILC (Majedova, 2003). There was no significant difference between the parent bentonite and NaOH/bentonite. The Na_2O introduced could have been on the surface of the bentonite or between the aluminosilicate layers. The FTIR results showed that the parent structure of bentonite remained intact after pillaring.

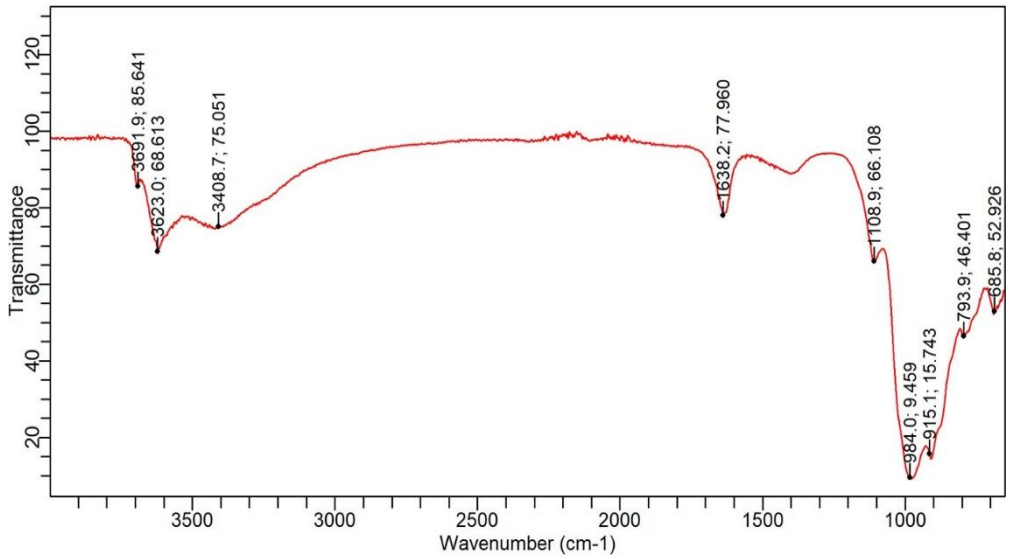

Figure 1. FTIR result of Bentonite

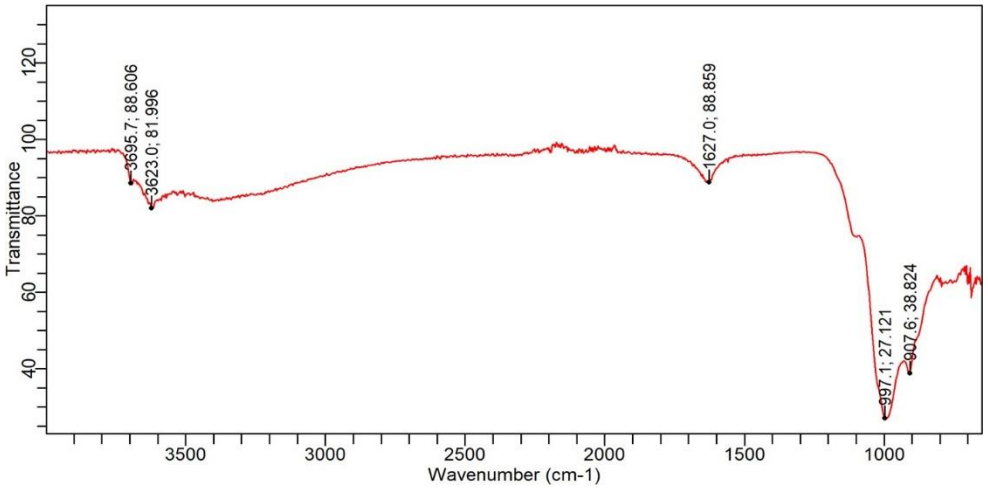

Figure 2: FTIR result of Al-PILC

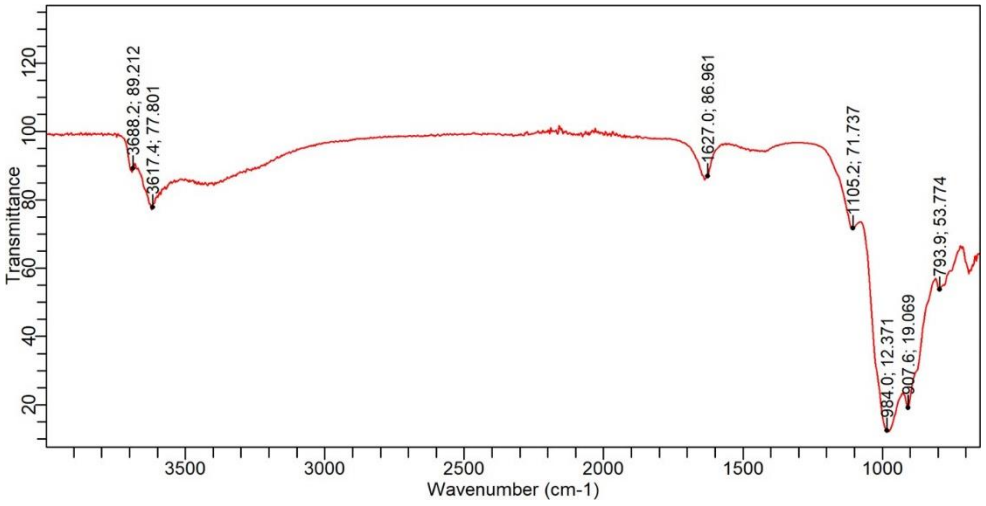

Figure 3: FTIR result of NaOH/Bentonite

Table 3: Result of XRD Analysis of Bentonite, Al-PILC and NaOH/Bentonite

Sample	2θ (^{0})	Basal d-spacing (d_{001})
Bentonite	6.99	12.65
Al-PILC	5.36	16.49
NaOH/Bentonite	7.10	12.45

The XRD result showed the samples contain phases of minerals such as montmorillonite which is the most prominent, quartz, calcite and muscovite (Masindi *et al*., 2015; Masindi *et al*., 2016). The success of a pillaring process can be confirmed using the basal spacing (d001). An increase in the basal spacing (d001) observed in the result is an indication of successful intercalation of Al oxides between the aluminosilicate layers of the montmorillonite. The basal spacing (d001) of the samples is listed in (Table 3). Patterns of bentonite and pillared clay in the XRD result revealed a shift of basal spacing (d001) from 2θ = 6.99^0 to 2θ = 5.36°. This matches to the increase in the basal d-spacing values of the raw bentonite from 12.65 to 16.49 Å for the pillared clay. This is also due to the formation of the pillars (Baloyi *et al*., 2019). Since there is a shift of the basal peak of the bentonite to lower 2 theta values, it can be also attributed to the successful formation of pillars by the active metal oxides through the cation exchange process (Fatimah, 2014). After impregnation with NaOH, the d001 values decreased, which translates to a reduction in the surface area, as shown in Table 4. The pillared clay constituents inherited the mineral phases in the bentonite. Therefore, pillaring process did not strongly affect the major structure of the starting clay.

Table 4: Result of Surface Area and Pore Volume Analysis

Sample	Surface Area (m^2/g)	Pore Volume (cc/g)	Pore diameter (nm)
Bentonite	302.1	0.186	2.132
Al-PILC	366.4	0.189	2.128
NaOH/Bentonite	267.2	0.161	2.139

The porosity and BET surface area of all the samples were determined using N_2 adsorption-desorption measurements. (Table 4). The pore volume and the surface area of Al-PILC were better than the values for the starting bentonite clay. The surface area and pore volume increased from 302.1 to 366.4 (m^2/g) and from 0.186 to 0.189 (cc/g), respectively. This showed that the pillaring has resulted in an increase in porosity and BET surface area. These results confirm the successful intercalation of Al polyoxycations into bentonite clay layers (Baloyi et al., 2019). The surface areas and pore volumes of the pillared clay reported by Muñoz *et al*. (2017); Moma *et al*. (2018) and Bolayi *et al*. (2019) were all lower than those reported here. The surface area and pore volume of NaOH/bentonite are lower than those of the parent clay, which points to a certain level of pore blockage and surface occupation by the new species (Hadjlraef *et al*., 2015). This decrease in surface area and pore volume is not peculiar because Ravari *et al*. (2020) and Hadjlraef *et al*. (2015) reported a decrease in pore volume surface area when CuO was impregnated into aluminium pillared clay. Similarly, Wang *et al*. (1998) reported a reduction in pore volume and surface area when NiO was loaded onto pillared clay. All the samples have a pore diameter within the range of 2.128 to 2.139 nm.

Table 5: Biodiesel yield

Catalyst	Yield (%)
Bentonite	69 ± 0.91
Al-PILC	71 ± 1.27
NaOH/Bentonite	83 ± 1.80

The biodiesel yields obtained are shown in Table 5. The yield was in the order of bentonite<Al-PILC< NaOH/bentonite. This indicates that the introduction of Na_2O plays an important role in facilitating transesterification. All catalysts gave an appreciable yield, which could be improved by optimizing the process.

Table 6: GC-MS fatty acid methyl ester compositions of biodiesel produced

Systematic Name	Peak Area (%)
Methyl tetradecanoate	0.20
Methyl hexadecanoate	8.23
Methyl 9-12-Octadecadienoate	3.60
Methyl 9-octadecenoate	43.0
Methyl Stearate	2.40
Methyl Eicosapentaenoate	6.24
Methyl docosanoate	1.99
Metyl tetracosanoate	1.97
Methyl dihydoxy-9-Octadecanoate	13.97

Table 6 shows the profiles methyl esters of biodiesel obtained from WCO using NaOH/bentonite (highest yield). The main methyl esters present in the biodiesel produced are that of octadecenoic acid (oleic acid) and dihydroxy octadecanoic acid (hydroxy stearic acid) that account for 56.97 % of the produced biodiesel. The esters of hexadecenoic (palmitic) and octadecanoic (stearic) acids, also account for 10.63 %. The methyl esters reported here are common in biodiesels obtained from many oils (Borugadda and Goud, 2012; Ma and Hanna, 1999). The biodiesel produced using the other two catalysts gave similar fatty acid methyl ester content. The biodiesel produced will not experience cold filter plugging point (CFPP) problems due the absence of polyunsaturated fatty acids. However, oxidation and polymerization will affect its storage stability because of the unsaturation. (Muhammad *et al*., 2016).

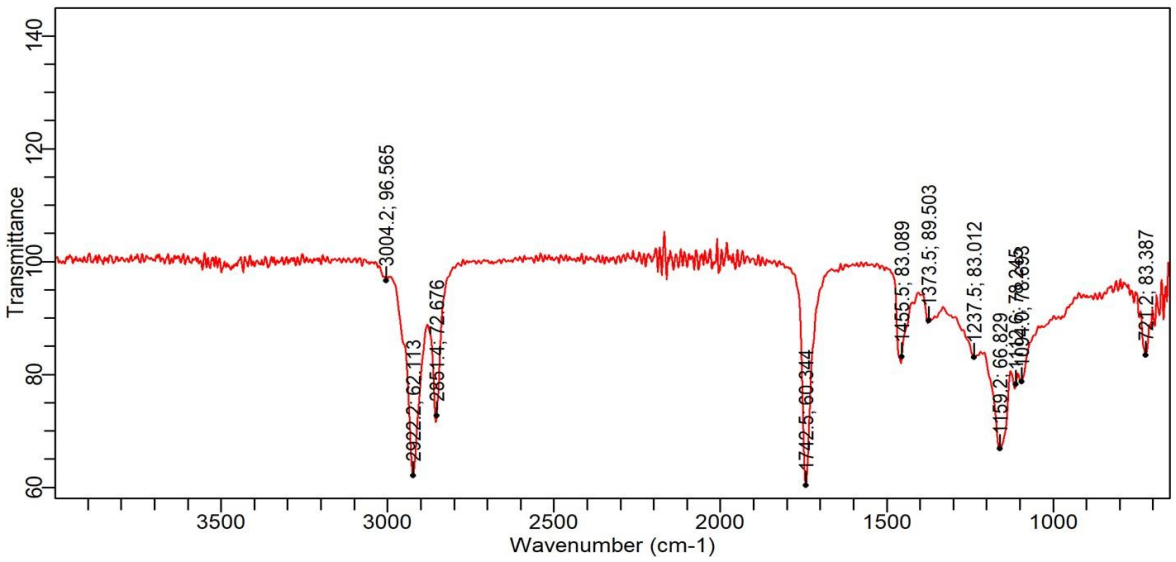

Figure 4: Representative FT-IR spectra of biodiesel samples

The FT-IR spectra of all the biodiesel followed the same pattern (Fig. 4). Bands that can be linked to the stretching of C = O are observed in the region from 1800-1700 cm^{-1}, which is characteristic of esters and is common in biodiesel and WCO (Sabrina *et al*., 2015). The "fingerprint" region (1500-900 cm^{-1}) can be used to distinguish between the WCO and the biodiesel. The asymmetric stretching of -CH_3 is represented by the band at 1455 cm^{-1} while the band at 1159 cm^{-1} represents the stretching of O-CH3 and is common in biodiesels (Sabrina *et al.*, 2015).

Table 7: Fuel properties of biodiesel obtained from WCO

Properties	Values	ASTM D6751-06a
Acid value (mg KOH/g)	0.66 ± 0.14	≤ 0.5 max
Saponification value (mg KOH/g)	187.04 ± 0.25	—
Iodine Value (gI_2/100 g)	77.15 ± 0.27	130max
Kinematic viscosity @ 40°C (mm2/s)	5.79 ± 0.00	1.90 – 6.00
Cetane Number	58.13 ± 0.89	47-65
High heating Value (MJ/kg)	40.60 ± 0.00	—

Free fatty acids present in a fuel can cause corrosion. It is important to measure the acid value of the biodiesel produced. The biodiesel's acid value (0.76 ± 0.14 mgKOH/g) exceeds the standard and the value reported by Muhammad *et al*. (2016). This indicates the need to reduce the acid level to a safe level. The amount of saponifiable fatty acid is measured by the saponification value. A high amount saponifiable fatty acids is indicated by the value obtained (187.04 ± 0.25 mgKOH/g) which is higher than the value 183.66 mgKOH/g) conveyed by Sokoto *et al*. (2011) but lower than the 190 mgKOH/g reported by Sani *et al*. (2017). This indicates a good quality for fuel production. The iodine value shows the average degree of unsaturation. From the value obtained (77.15 ± 0.27). It is evident that the biodiesel has a moderate degree of unsaturation, and it is within the stipulated limit. The resistance to the flow of a fluid under gravity is referred to as Kinematic viscosity. Vegetable oils have high viscosity which prevents their direct use in diesel engines. (Surachai, 2015). It is an important parameter to consider because fuels with high viscosity need strong thrusting into the ignition or compression chambers of several engines (Rabie *et al*., 2018). Kinematic viscosity obtained in this work at 40 ^{0}C (5.79 ± 0.00) which is within the acceptable range given by ASTM D6751. The quality of ignition of a fuel used can be specified using a cetane number. It is the measure of the time interval between the ignition delay time and injection of the fuel into the cylinder. The higher the cetane number the better because it shortens the ignition delay time. Unsaturation decreases the cetane number while it increases with increasing chain length (Gopinath *et al*., 2015). The cetane number obtained here is 58.13 ± 0.89 which is appreciable and within the standard limit. When complete combustion of one unit (kg/l m^3) of fuel occurs and heat is recovered from water vapour, the total amount of energy liberated is refer to as the higher heating value. It decreases with increasing unsaturation while increases with increasing chain length. (Gopinath *et al*., 2014). The HHV obtained here is appreciable (40.60 ± 0.00).

CONCLUSION

The present work was designed to prepare and characterize aluminium pillared clay and NaOH/bentonite for the transesterification of WCO into biodiesel. The XRF analysis revealed the presence of oxides in all the samples, with SiO_2 being the highest oxide in the samples. The amount of CaO is prominent as compared to K_2O and Na_2O, which indicates that the bentonite herein is calcium bentonite. The amount of Al_2O_3 increased while the interlayer cations decreased after pillaring, while Na_2O was observed after impregnation with NaOH. The FTIR result revealed prominent bands that were attributed to bentonites. The pillaring and impregnation of NaOH onto the bentonite caused some peaks to experience a reduction in their intensity, but the parent clay structure was maintained. The nitrogen adsorption-desorption measurements revealed that the BET surface area and pore volume increased significantly after pillaring. The XRD data showed an increase in basal d-spacing of bentonite after pillaring with kegging ions. Based on the foregoing, the pillared bentonite and the NaOH/Bentonite catalyst were successfully prepared, characterized, and tested for transesterification of WCO. All catalysts have shown transesterification ability, with NaOH/bentonite giving the highest yield (83 ± 1.80%) and methyl 9-octadecenoate as the most prominent fatty acid methyl ester.

ACKNOWLEDGEMENTS

The authors are grateful to Tertiary Education Trust Fund (TETFUND) for funding this research as part of the Institution-Based Research Intervention through Federal University Birnin Kebbi, Nigeria. TETF/DR&D/CE/UNIV/KEBBI/IBR/2022/VOL.1

REFERENCES

Abdul Raqeeb M. and Bhargavi R. (2015). Biodiesel production from waste cooking oil. *Journal of Chemical and Pharmaceutical Research*, **7**(12):670-681

Baloyi, J., Ntho, T. and Moma, J. (2019). Synthesis of highly active and stable Al/Zr pillared clay as catalyst for catalytic wet oxidation of phenol. *Journal of Porous Materials*, ***26***(2), 583–597. https://doi.org/10.1007/s10934-018-0667-3

Banerjee N. and Ritica R. and Tushar J. (2014). Biodiesel Production from Used Vegetable Oil Collected from Shops Selling Fritters in Kolkata. *Energy Procedia*, **54**, 161 – 165.

Borugadda V.B. and Goud V.V. (2012). Biodiesel production from renewable feedstocks: Status and opportunities. *Renew Sust Energ Rev*. **16:**4763–4784.

Collin, S. M. A., Wan, G. J., Ashri, M., and Wan, B. (2015). Preparation and characterization of activated carbon from Typha orientalis leaves. *International Journal of Industrial Chemistry* 6(1):9-21. https://doi.org/10.1007/s40090-014-0027-3

Daroughegi B. M., Hayati-Ashtiani M., Rezaei M. (2018) Preparation of pillared nanoporous bentonite and its application as catalyst support in dry reforming reaction. *Asia-Pac J Chem Eng*., **9**, 2188.

Elfadly A.M., I.F. Zeid, F.Z. Yehia, M.M. Abouelela, A.M. Rabie (2017) Production of aromatic hydrocarbons from

catalytic pyrolysis of lignin over acid-activated bentonite *clay Fuel Processing Technology*, **163:** 1–7

Farooq M., Anita R. and Abdul N. (2015) Biodiesel production from low FFA waste cooking oil using heterogeneous catalyst derived from chicken bones. *Renewable Energy*, 76, 362-368.

Fatimah I. (2014). Preparation of ZrO2/ Al2O3-montmorillonite composite as catalyst for phenol hydroxylation. *J. Adv. Res.* **5**, 663–670.

Galadima M.A., Dabai M.U., Bilyaminu R. A. and Jamilu I.U. (2022). Utilization of Waste Foil and Carbide Slag as Heterogeneous Catalyst for *In-Situ* Transesterification Of *Ricinus Communis* (Castor Seeds), *FUDMA Journal of Sciences*, **6**(6): 303-310

Gopinath, A., Sairam, K., Velraj, R., and Kumaresan, G. (2015). Effects of the properties and the structural configurations of fatty acid methyl esters on the properties of biodiesel fuel: A review. In *Proceedings of the Institution of Mechanical Engineers, Part D: Journal of Automobile Engineering* **22** (3): 357–390.

Hadjltaief, H. B., Zina, M. Ben, Galvez, M. E. and Da Costa, P. (2015). Photo-Fenton oxidation of phenol over a Cu-doped Fe-pillared clay. *Comptes Rendus Chimie*, ***18***(10), 1161–1169. https://doi.org/10.1016/j.crci.2015.08.004

Hamzah Noraini, Izyan Yusof, Wan Zurina Samad, Sabiha Hanim Saleh, Nazrizawati Ahmad Tajuddin, Mohd Lokman Ibrahim (2021). Production of Biodiesel from Waste Cooking Oil Using Bentonite. *Catalysts Journal of Academia*, **9**(1) 139 – 144

Kurian M. and Kavitha S. (2016) A Review on the Importance of Pillared Interlayered Clays in Green Chemical Catalysis. *IOSR Journal of Applied Chemistry*, **9**, 47-57.

Liu L. and Corma A. (2018). Metal Catalysts for Heterogeneous Catalysis: From Single Atoms to Nanoclusters and Nanoparticles. *Chemical Reviews*, **118**: 4981–5079.

Ma F. and Hanna M.A. (1999). Biodiesel production: A review. *Bioresour Technol*. **70**:1–15.

Madejova J. (2003). FTIR techniques in clay mineral studies, *Vib. Spectrosc*. **31**:1–10.

Masindi V., Gitari M.W., Tutu H. and DeBeer M. (2015). Synthesis of cryptocrystalline magnesite–bentonite clay composite and its application for neutralization and attenuation of inorganic contaminants in acidic and metalliferous mine drainage. *J. Water Process Eng*. **15**, 233-242.

Masindi V., Gitari W.M. and Pindihama K.G. (2016). Synthesis of cryptocrystalline magnesite/bentonite clay composite and its application for removal of phosphate from municipal wastewaters. *Environ. Technol*. **37**, 603–612.

Moma, J., Baloyi, J.and Ntho, T. (2018). Synthesis and characterization of an efficient and stable Al/Fe pillared clay catalyst for the catalytic wet air oxidation of phenol. *RSC Advances*, ***8***(53), 30115–30124.

Muhammad, A.B., Obianke, M., Gusau, L.H. and Aliero, A.A. (2016). Optimization of Process Variables in Acid Catalysed *In-Situ* Transesterification of *Hevea Brasiliensis* (Rubber Tree) Seed Oil into Biodiesel. *Biofuels*, **8:** 585-594.

Muñoz, H. J., Blanco, C., Gil, A., Vicente, M. ángel, and Galeano, L. A. (2017). Preparation of Al/Fe-pillared clays: Effect of the starting mineral. *Materials*, ***10***(12), 122-36 https://doi.org/10.3390/ma10121364

Ofoegbu-Chibuzo, N. E., Chukwu, U. J., & Okoye, I. P. (2022). Characterization of Natural Ca-Bentonite Clays from Ebenebe in Anambra State, Nigeria, Impregnated with Ca(NO3)2, Zn(NO3)2 and KOH for use as Catalysts for Viscosity Reduction in Transesterification Reaction of Castor Oil. *Journal of Applied Sciences and Environmental Management*, ***26***(11),1827–1833. https://doi.org/10.4314/jasem.v26i11.14

Rabie, A. M., Mohammed, E. A., and Negm, N. A. (2018). Feasibility of modified bentonite as acidic heterogeneous catalyst in low temperature catalytic cracking process of biofuel production from nonedible vegetable oils. *Journal of Molecular Liquids*, ***254***, 260–266.

Rahadianti E. S., Yerizam and Martha (2018). Biodiesel Production from Waste Cooking Oil**.** *Indonesian Journal of Fundamental and Applied Chemistry* **3**(3), 77-82

Ravari, M. H., Sarrafi, A. and Tahmooresi, M. (2020). Synthesizing and characterizing the mixed Al,Cu-pillared and copper doped Al-pillared bentonite for electrocatalytic reduction of CO2. *South African Journal of Chemical Engineering*, **31**, 1–6. https://doi.org/10.1016/j.sajce.2019.10.001

Sabrina N. R., Vany P. F., Leandro S. O. and Adriana S. F. (2015). FTIR Analysis for Quantification of Fatty Acid Methyl Esters in Biodiesel Produced by Microwave-Assisted Transesterification. *International Journal of Environmental Science and Development*, **6**(12), 964-969

Saini R. D. (2017). Conversion of Waste Cooking Oil to Biodiesel. *International Journal of Petroleum Science and Technology* **11**(1): 9-21.

Sani, J., Sokoto, A. M., Tambuwal, A. D., and Garba, N. A. (2017). Effect of NiO/SiO2 on thermo-chemical conversion of waste cooking oil to hydrocarbons. *Heliyon*, **3**, 304.

Sokoto, M.A., Hassan, L.G., Dangoggo, S.M., Ahmad, H.G., Nasir, J., Salleh, M. A., (2011). Effect of catalyst concentration and temperature on transesterification of oil extracted from the Curcubita pepo (pumpkin) seeds. *Nigerian Journal of Renewable Energy*, **16**, 57–63.

Suhas P. Suhas, Veda Ramaswamy, A.V. Ramaswamy (1999) Ultrasonification: a competitive method of incerlation for the preparation of alumina pillared montmorillonite catalyst. *Catalysis Today* **49**: 313-320.

Surachai, J. (2015). Preparation of Vegetable Oil as Biodiesel Feedstock via Re- esterification: A Suitable Catalyst. *Energy Procedia* **79**, 143–148.

Tadesse, A. D., Tadios,T. M.and Yedilfana, S. M. (2019) Optimized Biodiesel Production from Waste Cooking Oil (WCO) using Calcium Oxide (CaO) Nanocatalyst. **9**, 18982

Trombetta M., Busca G., Lenardab M., Storaro L., Ganzerla R., Piovesan L., Jimenez A. L., Alcantara-Rodriguez M. and Rodriguez-Castellón E. (2000) Evaluation of surface acidity of mono- and bi-pillared smectites by FT-IR spectroscopy measurements, NH3-TPD and catalytic tests. *Applied Catalysis A:General,* **193**:55–69

Wang, S., Zhu, H. Y., & Lu, M. (1998). Preparation, Characterization, and Catalytic Properties of Clay-Based Nickel Catalysts for Methane Reforming. In *Journal Of Colloid And Interface Science*. 204

Zhang H., Jincheng D., and Zengdian Z. (2012). Microwave-assisted esterification of acidified oil from waste cooking oil by CERP/PES catalytic membrane for biodiesel production. *Bioresource Technology* 123, 72–77.

Zhou, J., Wu, P., Dang, Z., Zhu, N., Li, P., Wu, J., & Wang, X. (2010). Polymeric Fe/Zr pillared montmorillonite for the removal of Cr(VI) from aqueous solutions. *Chemical Engineering Journal*, **162**(3), 1035–1044.